

Conduction properties of $a\text{-Si:H } n^+ \text{-}i \text{-}n^+$ structures: Analysis taking into account the effects of $n^+ \text{-}i$ space-charge regions

G. de Rosny

Groupe de Physique des Solides, Université Paris VII, 2 place Jussieu, 75251 Paris CEDEX 05, France

B. Equer and A. Labdi

Laboratoire de Physique des Interfaces et des Couches Minces, Ecole Polytechnique, 91128 Palaiseau, France

(Received 28 February 1991; revised manuscript received 30 January 1992)

The analysis of I - V characteristics of sandwich $a\text{-Si:H } n^+ \text{-}i \text{-}n^+$ structures is performed, taking into account the effects of the $n^+ \text{-}i$ space-charge regions. This enables the computation of the characteristics from the low-bias-linear to the space-charge-limited current regimes, for arbitrary intrinsic layer thicknesses. In the usual analysis, where the influence of $n^+ \text{-}i$ interfaces is neglected, a scaling law is expected to hold for thick enough i layers. In the present work, the validity of this law is checked as a function of the Fermi-level density of states (DOS). For instance, it is found that the scaling law does not hold for a $4\text{-}\mu\text{m}$ -thick i layer with a $10^{15} \text{ cm}^{-3} \text{ eV}^{-1}$ Fermi-level DOS. The I - V measurements on a set of four samples of various thicknesses and a single intrinsic material quality are fairly well described by the model, using a unique Fermi-level DOS value and slope. These two parameters are strongly constrained by the requirement to describe simultaneously the I - V measurements on thin and thick samples.

I. INTRODUCTION

The space-charge-limited current (SCLC) method has been widely applied in the past ten years to the study of deep-gap states' density in amorphous semiconductors. In particular, it is commonly applied to investigate the density of states of intrinsic amorphous silicon and silicon-carbon, silicon-germanium alloys or silicon nitrides using $n^+ \text{-}i \text{-}n^+$ structures. Different analyses of the current-voltage (I - V) measurements have been developed. They are addressing different problems, and two approaches can be separated as follows. (a) Direct calculations aiming to compute the (I - V) function either for different types of density of states¹ (one gap state, constant density of states, etc.) or for different kinds of physical hypotheses as, for example, nonhomogeneous layers,² inclusion of conduction mechanism such as diffusion,³ or high electric field (Poole-Frenkel) (Refs. 3 and 4). (b) Inverse calculation, i.e., techniques which start from the experimental (I - V) curves joined to well-defined physical hypotheses and allow one to extract the density of states at the Fermi level, or to estimate the shape of the density of states above and in the vicinity of the Fermi level.³

From direct calculations, and using a set of physical hypotheses which we will call "standard conditions," namely, (i) only electrons contribute to the current; (ii) local thermal equilibrium among electrons, at the sample temperature, is achieved; (iii) the injecting $n^+ \text{-}i$ interface does not limit the electron current, some general predictions can be made. As a matter of fact, if the diffusion current is neglected, the following four basic quantities: the current I , the voltage V , the electric field $F(x)$, and the density of free carriers $n(x)$, are related by three simple equations: current conservation, the Poisson equation,

and the relation between V and $F(x)$. The density of charged traps is involved in the Poisson equation, but can always be related to the $n(x)$ using condition (ii). One can easily show that the system obeys a "scaling law" with respect to the layer thickness t : replacing x by $u = x/t$, F by $f = F/t$, V by $v = V/t^2$, and I by $i = I/t$ leads to equations giving $f(u)$, v , and $n(u)$ for a given i . Taking condition (iii) into account allows one to prove that there is a universal relation between i and v , given a density of deep states, or in other words that I/t is a function of V/t^2 , whatever the value of t . A more elegant proof makes use of no-dimension variables.¹ This law can be experimentally checked⁶ and is often used as a means to verify that samples do not present any spurious effect like a serial Schottky diode at one of the electrode- n^+ interfaces.

Inverse calculations stem directly from the direct ones in the case where assumptions made on the density of states allow a direct, analytical extraction of at least one physical quantity, i.e., the Fermi-level density of states N_F .⁵⁻⁷ For example, one predicts the result $I/t \propto (V/N_F t^2) \exp(\epsilon \epsilon_0 V / q N_F t^2)$, in the case of a constant density of states.

Apart from a few cases, some numerical computations need to be performed to obtain the (I - V) relation. For example, solving the standard SCLC equations for an exponential density of states⁶ leads to a series which can be numerically summed and the resulting curves compared to the experimental ones to find N_F . For more general density-of-states (DOS) profiles, the inverse problem was solved and two relations were established: one between the DOS profiles $N_{\text{DOS}}(E-E_F)$ and the three first derivatives of the (I - V) relation and the other one between ($E-E_F$) and the same derivatives.³ Applied to amor-

phous silicon experimental (I - V) curves, this allows one to extract the DOS profile for a range of energies extending 100 meV above Fermi level. However, the method is very sensitive to experimental errors and to the numerical procedure used to extract successive derivatives.

Whatever the method used, the physical quantities deduced from experimental results reflect both material properties and physical assumptions stated as the basis of each method. Although some insight can be given into the role of phenomena not taken into account in the standard conditions, it is the aim of this paper to formulate and solve the SCLC in a somewhat larger frame of hypothesis taking into account the effects of $n^+ \text{-}i$ interfaces and of i layer thickness. The underlying physical assumptions are similar to the ones introduced by Bonham to analyze hole transport in polymers;⁷ they have also been introduced by Meaudre to analyze $a\text{-Si:H}$ film thickness dependence of the Ohmic conductivity.⁸

II. COMPUTATION OF THE J - V CHARACTERISTICS

A. Physical assumptions

In this section the physical assumptions introduced are described and the set of equations allowing the computation of I - V characteristics is derived. Among the assumptions, some may be viewed as essential, in the sense that one cannot relax one of them without changing completely the modelization, other ones are introduced for sake of simplification but might be modified if necessary within the framework of the model. It must be understood that the $n^+ \text{-}i\text{-}n^+$ structure, actually a $m\text{-}n^+ \text{-}i\text{-}n^+ \text{-}m'$, m and m' being metal layers, is of sandwich type, the potential bias V being applied to the metal layers connecting the n^+ layers to the measurement apparatus, with the current I flowing normally to the layers boundaries. In all the following one will be concerned uniquely with time-independent phenomena.

The physical hypotheses essential for the modelization may be expressed as follows: (a) the *films are uniform* in the directions parallel to their boundaries; (b) only *electrons* contribute to the current; (c) in the whole structure, the electrons are in local thermal equilibrium, at the measurement apparatus temperature T . One may then introduce an electron pseudo-Fermi energy level to describe the electron states' occupancies; it will hereafter be denoted $E_F(x)$. (d) The electron current density J may be expressed in terms of conduction and diffusion as follows:

$$J = q\mu n(x)F(x) + qD \frac{dn(x)}{dx} .$$

x is the abscissa of a point in the intrinsic layer, in a direction perpendicular to the interfaces. q is the elementary charge, μ the conduction-band electron mobility, $n(x)$ the conduction-band electron density, $F(x)$ the electric field, and D the electron diffusion coefficient. The mobility μ is assumed field independent and linked to the diffusion coefficient D by the Einstein relation $D = kT\mu/q$. (e) The electron density of states is position independent in the intrinsic layer. This may be wrong as

one suspects that the $a\text{-Si:H}$ structure may be influenced by the proximity of interfaces. Indeed in some cases, the observation of a failure of scaling in SCLC measurements when using rather thin samples has been attributed to an increase of DOS in the vicinity of interfaces.^{6,9} It is possible that the departure from scaling is, at least partly, a consequence of the inadequacy of the standard conditions for these thin samples. (f) The potential drop takes place uniquely in the intrinsic layer. As a consequence, the electron quasi-Fermi level $E_F(x)$ coincides with the n^+ layers Fermi levels at the $n^+ \text{-}i$ boundaries. This constitutes a simplifying assumption, which may be to some extent relaxed if necessary.

B. Derivation of the transport equation

From the above hypotheses, the quantities convenient to evaluate the J - V characteristic may be computed as a solution of a second-order differential equation with a given set of boundary conditions. Let us start from the Poisson equation:

$$\epsilon \frac{dF(x)}{dx} = \rho(x) ,$$

where ϵ is the $a\text{-Si:H}$ dielectric constant, and $\rho(x)$ the charge density. The electric field $F(x)$ is the opposite of the internal electrostatic potential gradient, which is itself linearly related to the electron conduction-band mobility energy $E_c(x)$:

$$F(x) = \frac{dE_c(x)}{qdx} .$$

Let

$$E_d(x) = E_c(x) - E_F(x) .$$

Whatever the charge state of an occupied level, the charge density may be evaluated if one notices that $\rho = 0$ for a bulk material at equilibrium, $E_d = E_{db}$, E_{db} being the distance between the conduction-band edge and the bulk Fermi level. Then the electron occupation probability differences of the states, between the bulk situation and another one characterized by a given value of E_d , integrated over the whole DOS distribution, gives the charge density:

$$\rho(E_d) = -q \int g(E) [f(E, E_d) - f(E, E_{db})] dE .$$

E is the energy of a state, referenced to the conduction-band edge. $f(E, E_d)$ is the state occupation probability, which depends only on the difference $E - E_d$, and $g(E)$ is the DOS distribution; the integration extends in principle to the whole energy range, but is in practice limited to the energies where the difference between the occupation probability functions is appreciably different from 0.

From the fact that the charge density depends on the position only through $E_d(x)$, the Poisson equation may be written

$$\frac{d^2 E_c(x)}{dx^2} = -\frac{q}{\epsilon} \rho(E_d(x)) ,$$

which may be rewritten taking into account that $E_c(x) = E_F(x) + E_d(x)$

$$\frac{d^2 E_F(x)}{dx^2} + \frac{d^2 E_d(x)}{dx^2} = -\frac{q}{\epsilon} \rho(E_d(x)) .$$

Charge conservation implies that the current density J is position independent. Owing to the nondegeneracy hypothesis, one may express the current density as follows:

$$J = \mu n(x) \frac{dE_F(x)}{dx}$$

or equivalently

$$J = \mu N_c \exp \left[\frac{-E_d(x)}{kT} \right] \frac{dE_F(x)}{dx} .$$

One may then eliminate $E_F(x)$ between the Poisson equation and this last one to get a second-order differential equation in $E_d(x)$:

$$\frac{d^2 E_d(x)}{dx^2} + \frac{J}{\mu N_c kT} \exp \left[\frac{E_d(x)}{kT} \right] \frac{dE_d(x)}{dx} = \frac{q}{\epsilon} \rho\{E_d(x)\} . \quad (1)$$

According to assumption (f) above, at the $n^+ - i$ boundaries E_d is equal to the difference between the conduction band and the Fermi energies in the n^+ material, which is also the n^+ material activation energy E_a^+ .

Choosing the origin of the abscissa at one interface and calling t the intrinsic layer thickness, the boundary conditions may be written

$$E_d(0) = E_d(t) = E_a^+ .$$

For a given current density, it is then possible to compute $E_d(x)$ and then the potential bias V , related to the Fermi-level difference between the two n^+ layers.

$$V = -\frac{E_F(t) - E_F(0)}{q} ,$$

this may be expressed as

$$V = -\frac{J}{q\mu N_c} \int_0^t \exp \left[\frac{E_d(x)}{kT} \right] dx . \quad (2)$$

C. Variable change for numerical evaluations

The second-order differential equation satisfied by E_d does not depend explicitly on the position x ; it is then possible to reduce it to a first-order equation. Let us introduce the dimensionless variable u defined as

$$u(x) = \exp \left[\frac{E_d(x)}{kT} \right]$$

and let

$$u'(x) = \frac{du(x)}{dx} .$$

Then Eq. (1) may be rewritten as follows:

$$\frac{d}{dx} \left[\frac{u'}{u} \right] + Mu' = \frac{q}{\epsilon kT} \rho(u) ,$$

where

$$M = \frac{J}{\mu N_c kT} .$$

Noting that $d/dx = u'(d/du)$, one may write

$$\frac{u'}{u} \frac{d}{du} \left[\frac{u'}{u} \right] + M \frac{u'}{u} = \frac{q\rho(u)}{\epsilon kT u} .$$

Finally define

$$Z = \frac{u'}{u} , \quad Z' = \frac{dZ}{du} .$$

The equation may be written in the final form

$$ZZ' + MZ = -R(u) , \quad (3)$$

with

$$R(u) = -\frac{q}{\epsilon kT} \frac{\rho(u)}{u} .$$

In the present situation of electron injection, $\rho(u)$ is negative, so that $R(u)$ is positive.

At the intrinsic layer boundaries,

$$u = u_0 = \exp \left[\frac{E_a^+}{kT} \right] .$$

According to the nature of the $N^+ - I$ interfaces, it is assumed that u is minimal at these boundaries, so that $u_0 \leq u$. Let u_m be the maximum value taken by u , at this position $Z = u'/u = 0$.

For a given u_m , Eq. (3) may be solved, leading to the determination of Z between u_m and u_0 ; it turns out that Z is a bivaluated function of u , one branch corresponding to $Z > 0$, call it $Z_+(u)$, and the other one to $Z < 0$, call it $Z_-(u)$. These two branches correspond to the two regions of the intrinsic layer on both sides of the position t_m where $u = u_m$, Z_+ corresponds to $0 < x < t_m$, and Z_- to $t_m < x < t$.

One may now relate the applied bias V and the intrinsic layer thickness to Z_+ and Z_- . Equation (2) may be rewritten

$$V = -\frac{kTM}{q} \int_0^t u(x) dx .$$

Using the fact that $u dx = du/Z$ and separating the regions corresponding to the two solutions for Z , one gets

$$V = -\frac{kTM}{q} \int_{u_0}^{u_m} \left[\frac{1}{Z_+(u)} - \frac{1}{Z_-(u)} \right] du . \quad (4)$$

Similarly, the thickness is expressed as follows:

$$t = \int_{u_0}^{u_m} \left[\frac{1}{Z_+(u)} - \frac{1}{Z_-(u)} \right] \frac{du}{u} . \quad (5)$$

So the procedure to get the J - V characteristic is to as-

sume a value for J , assume a value for u_m , solve Eq. (3) for $Z_+(u)$ and $Z_-(u)$, compute V and t , then iterate on u_m until a convenient value of t is obtained.

D. Numerical procedure

To solve Eq. (3), the following procedure has been used.

(a) Decompose the $\{u_0, u_m\}$ interval into sections in which the function $R(u)$ may be regarded as constant; say that the relative variation of $R(u)$ is of about 1%.

(b) In each section solve Eq. (3) assuming $R(u) = R_a$, where R_a is the average value of $R(u)$ in the section.

(c) Starting from u_m , where Z is known to be equal to 0, join the solutions in each section by imposing that Z is continuous at the boundaries.

(d) Compute the contributions of each section for the evaluation of V and t , by Eqs. (4) and (5).

The solution of Eq. (3), with $R(u) = R_a = \text{const}$, may be expressed as follows: Define $Y = MZ/R_a$, then Eq. (3) leads to

$$\left[1 - \frac{1}{1+Y}\right] dY = -\frac{M^2}{R_a} du.$$

Let u_2 be the upper edge of the section, where $Z = Z_2$ and hence $Y = Y_2$ is known from the evaluation in the preceding section. Then Y in the section satisfies the relation

$$Y - \ln(1+Y) = Y_2 - \ln(1+Y_2) + \frac{M^2}{R_a}(u_2 - u). \quad (6)$$

The contribution of the section $\{u_1, u_2\}$ to the potential V is

$$V_{1,2} = -\frac{kTM}{q} \int_{u_1}^{u_2} \left[\frac{1}{Z_+(u)} - \frac{1}{Z_-(u)} \right] du$$

which, noting that

$$\frac{1}{Z} = -\frac{Y'}{M} - \frac{M}{R_a},$$

may be expressed as

$$V_{1,2} = \frac{kT}{q} \{Y_{+2} - Y_{+1} - Y_{-2} + Y_{-1}\},$$

where Y_+ and Y_- correspond, respectively, to Z_+ and Z_- and Y_1 is the value of Y at $u = u_1$.

The contribution of the $\{u_1, u_2\}$ interval to the thickness is

$$t_{1,2} = \int_{u_1}^{u_2} \left[\frac{1}{Z_+(u)} - \frac{1}{Z_-(u)} \right] \frac{du}{u}$$

or

$$t_{1,2} = \frac{M}{R_a} \int_{u_1}^{u_2} \left[\frac{1}{Y_+(u)} - \frac{1}{Y_-(u)} \right] \frac{du}{u}.$$

This integral has been evaluated numerically using ap-

proximations of the functions $Y_+(u)$ and $Y_-(u)$ satisfying Eq. (6) (see Appendix B).

E. Energy dependence of the charge density

Depending on DOS shape, some approximations may be introduced to evaluate the charge density. For the states belonging to the conduction band, one uses the standard effective level approximation, valid for nondegenerated semiconductors:

$$\rho_c(E_d) = -qn(E_d),$$

with

$$n(E_d) = N_c \exp(-E_d/kT),$$

where N_c is the conduction-band effective density of states.

The *a*-Si:H band-gap DOS is believed to be rather flat in the bulk Fermi-level vicinity; the occupation probability may then be approximated by a step function, which constitutes the 0-K approximation. But the DOS is observed to increase exponentially with energy faster than the drop of the Fermi-Dirac occupation probability¹⁰⁻¹² as the energy gets close to the conduction-band edge, a situation which cannot be accounted for by the 0-K approximation. The incidence of these states on the charge density is analyzed in Appendix A, where it is shown that the charge density may be evaluated assuming an effective number of gap states per unit volume at the conduction-band edge, let N'_c be this number, and a charge density $\rho_1(E_d)$ whose functional dependence is derived in Appendix A.

Using the 0-K approximation, for the DOS around the Fermi level, one then gets the expression for the charge density:

$$\rho(E_d) = -q \int_{E_d}^{E_{db}} g(E) dE - q \left[\frac{N'_c}{N_c} + 1 \right] \{n(E_d) - n(E_{db})\} + \rho_1(E_d),$$

where $n(E_{db})$ is the conduction-band electron density of the bulk material.

The DOS $g(E)$ is usually assumed either energy independent (flat) or to depend exponentially on E . In the latter case, one may write

$$g(E) = g(E_{db}) \exp \frac{E_{db} - E}{lkT}.$$

$g(E_{db})$ is the DOS at the bulk Fermi level, and l characterizes the DOS logarithmic slope with respect to the measurement inverse temperature. The 0-K approximation is valid only if $l > 1$.

III. RESULTS OF THE CALCULATIONS

The following sets of plausible parameters were introduced in a simulation program, written in Microsoft QUICK BASIC 4 language.

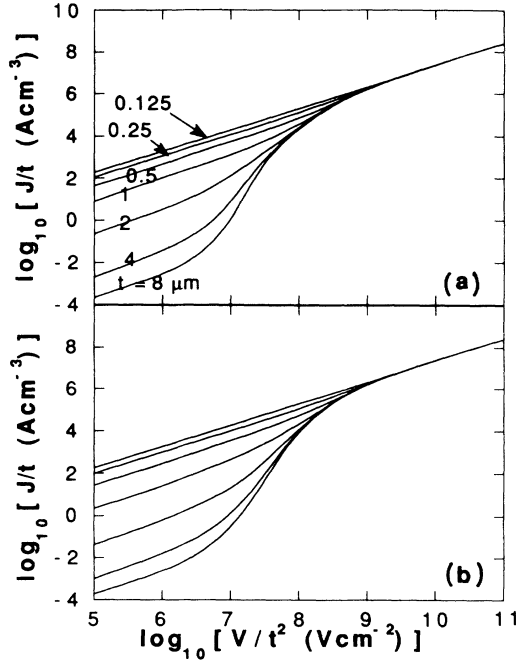


FIG. 1. J - V characteristics, in the scaling variable plane, for a $10^{15} \text{ cm}^{-3} \text{ eV}^{-1}$ Fermi-level DOS, flat (a) and slope $l=8$ (b).

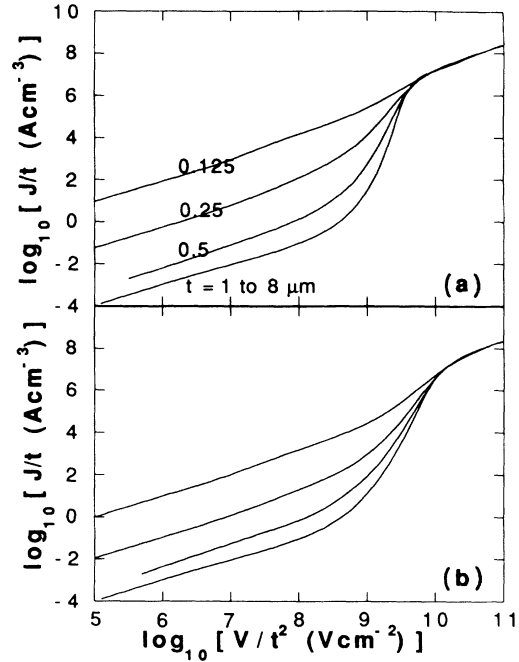


FIG. 3. J - V characteristics, in the scaling variable plane, for a $10^{17} \text{ cm}^{-3} \text{ eV}^{-1}$ Fermi-level DOS, flat (a) and slope $l=8$ (b).

N_c (cm^{-3})	μ_c ($\text{cm}^2 \text{V}^{-1} \text{s}^{-1}$)	$D_{cb} = N_c / kT$ ($\text{cm}^{-3} \text{eV}^{-1}$)	E_a^+ (eV)	E_{db} (eV)
2.6×10^{19}	30	10^{21}	0.28	0.67

(Please note that the last two numbers, 0.28 and 0.67,

were measured in the materials used in our samples.)

The calculation was performed for the following set of values: thicknesses: 8, 4, 2, 1, 0.5, 0.25, and 0.125 μm ; bulk Fermi-level DOS: 10^{15} , 10^{16} , and $10^{17} \text{ cm}^{-3} \text{ eV}^{-1}$; DOS slopes: flat, $l=8$, $l=3$.

Owing to the large number of simulation data, it is difficult to present them here extensively, so they are arranged to approach two questions of interest in SCLC measurements: one is the validity of the thick sample approximation, the second is the sensitivity of SCLC to the DOS slope.

A convenient way to study the validity of the thick sample approximation is to display the results in terms of "scaling variables" namely $J/t - V/t^2$, for which the characteristics should not depend on the sample thickness t . Figures 1–3 show the results. One observes in

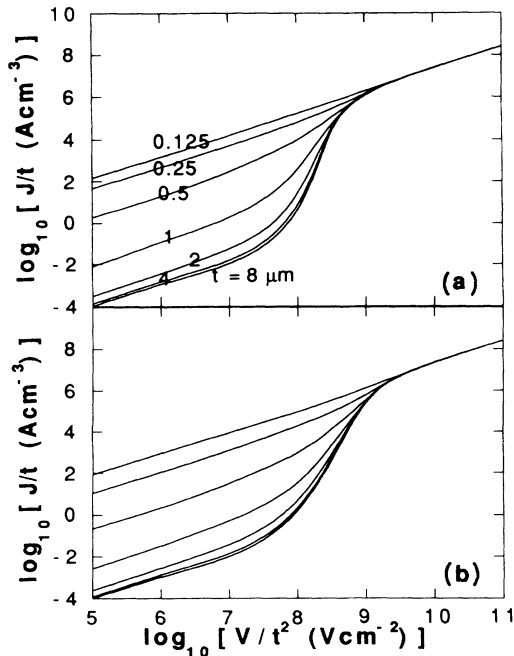


FIG. 2. J - V characteristics, in the scaling variable plane, for a $10^{16} \text{ cm}^{-3} \text{ eV}^{-1}$ Fermi-level DOS, flat (a) and slope $l=8$ (b).

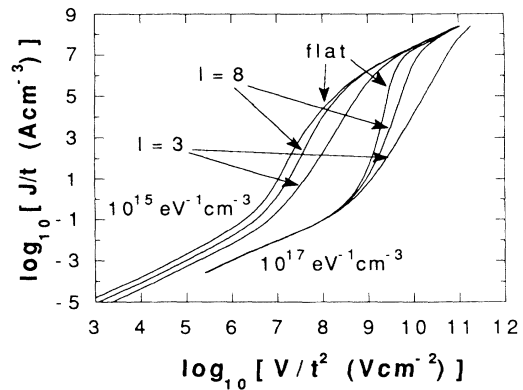


FIG. 4. J - V characteristics, in the scaling variable plane, of a 4- μm -thick sample with Fermi-level DOS values 10^{15} and $10^{17} \text{ cm}^{-3} \text{ eV}^{-1}$ and flat, $l=3$ or $l=8$ DOS slopes.

particular that the scaling law is not yet verified for 4- μm -thick samples, if the bulk Fermi-level DOS is equal to $10^{15} \text{ cm}^{-3} \text{ eV}^{-1}$.

At high current density, a scaling law with J proportional to V is observed; it corresponds to the situation where the electron injection is high enough to impose a density of conduction electrons independent of the position, and equal to the density at the $N^+ \text{-}I$ interfaces.

The sensitivity of SCLC to DOS slopes is illustrated in Fig. 4, displaying $J\text{-}V$ characteristics of a 4- μm -thick sample, with 10^{15} and 10^{17} states $\text{cm}^{-3} \text{ eV}^{-1}$ at the bulk Fermi level. For the lower DOS, where the scaling approximation does not hold, the conductance is slope dependent in the low- J region, where an Ohmic behavior is observed. This means that the contribution of the space-charge regions to the conductance is still significant.

The effect on the $I\text{-}V$ characteristics of the conduction-band edge tail states, which have been introduced in the simulations, is expected to be sizable only in the limit of low Fermi-level DOS. It turns out that, even for the lowest Fermi-level DOS hypothesis, namely $10^{15} \text{ eV}^{-1} \text{ cm}^{-3}$, the contribution of the tail states is marginal.

It may be of interest to visualize the evolution of the band shape as a function of the current density. In Fig. 5(a), the quantity $E_d(x) = E_c(x) - E_F(x)$ is drawn for a 2-

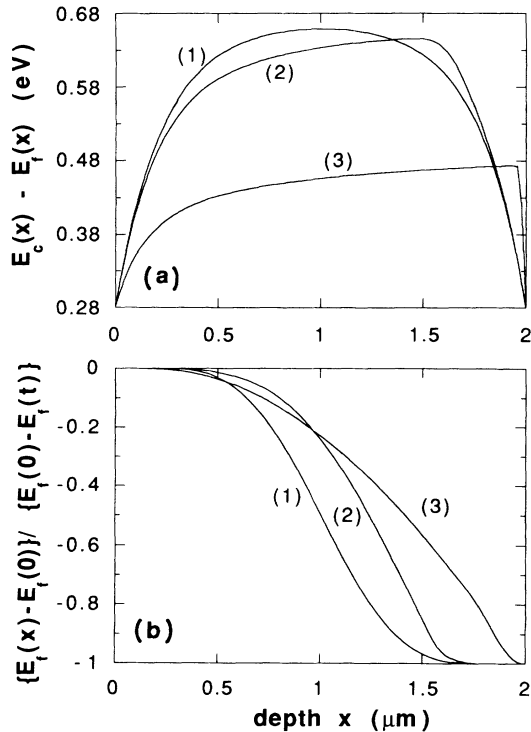


FIG. 5. Sample characteristics: thickness 2 μm , $10^{16} \text{ eV}^{-1} \text{ cm}^{-3}$ flat Fermi-level DOS. Polarization conditions (1): $J = 10^{-7} \text{ A cm}^{-2}$, $V = 6.5 \text{ mV}$; (2): $J = 10^{-5} \text{ A cm}^{-2}$, $V = 0.37 \text{ V}$; (3): $J = 0.1 \text{ A cm}^{-2}$, $V = 6.7 \text{ V}$. (a) Position dependence of the distance between the conduction-band edge and the pseudo-Fermi level. (b) Position dependence of the pseudo-Fermi level, normalized to its total variation.

μm -thick sample with a $10^{16} \text{ eV}^{-1} \text{ cm}^{-3}$ flat DOS at various current densities. The polarization is such that electrons are injected from the left. One observes an overall increase of the electron density in the sample as the current density is increased, especially in the region close to the cathode, and one observes also a diminution of the electron density, as compared to the equilibrium situation in the vicinity of the anode for a high enough current density.

The pseudo-Fermi-level position dependence, normalized to its overall variation, is displayed in Fig. 5(b). It is observed, as expected, that its slope is connected to the value of $E_d(x)$ displayed in Fig. 5(a).

IV. ANALYSIS OF EXPERIMENTAL DATA

$J\text{-}V$ characteristics have been measured on a set of samples made of the same intrinsic material, the thickness of it being varied. The material properties were as

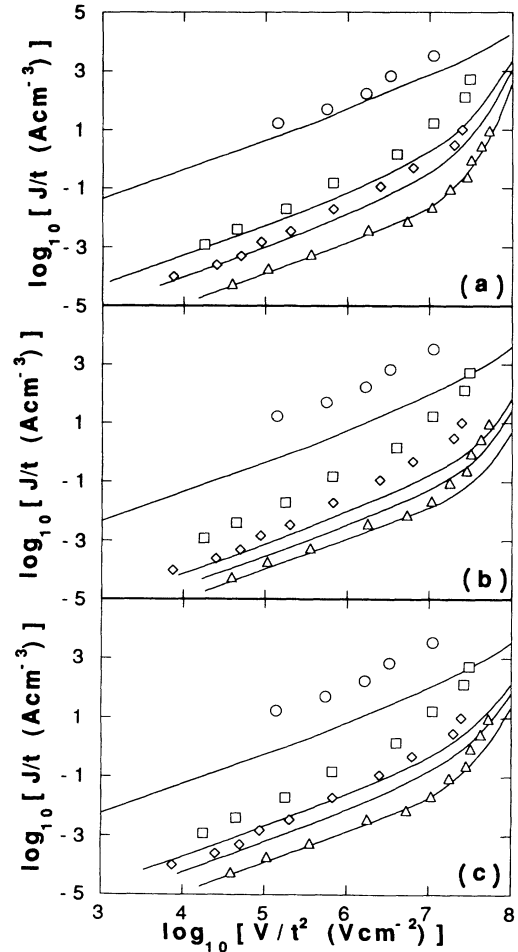


FIG. 6. $J\text{-}V$ characteristics in the scaling variable plane, measured on a set of samples made of the same I material and of thicknesses 5.3 (Δ), 2 (\diamond), 1.5 (\square), and 0.6 (\circ) μm and compared to the prediction of various Fermi-level DOS values (unit $\text{cm}^{-3} \text{ eV}^{-1}$) and slopes. (a) 4×10^{15} , flat; (b) 10^{16} , flat; (c) 4×10^{15} , $l = 8$.

much as possible maintained identical for each sample. Possible contamination of the i layer by phosphorus used to make the n^+ layers was minimized by the use of a reactor allowing the deposition of the two types of layers in separate chambers. It turned out that for thin samples, a contribution to the potential drop taking place at the metal- n^+ interfaces had to be subtracted in view to get the actual i layer bias. Details on the experimental procedures may be found in Refs. 13 and 14, where results on the J - V characteristics temperature dependences, in the low-bias-linear region, are also presented. It is shown that they may be well accounted for taking into account the influence of the n^+ - i charge space regions.

In Figs. 6(a)–6(c), the result of the model is compared with the J - V measurements. One observes that the best agreement is obtained for an energy-independent DOS with 4×10^{15} states $\text{cm}^{-3}\text{eV}^{-1}$. No systematic optimization of the parameters was attempted, but it appears that only a rather flat DOS can describe the whole set of measurements. If one considers only the thickest sample, one observes that the experimental measurements may be accounted for by various combinations of DOS densities and slopes, so that the measurements on thin samples bring a significant constraint to the values of the adjustable parameters.

V. DISCUSSION

The interpretation of the measurements excludes that the DOS exhibits a sizable exponential slope as a function of energy in the vicinity of the bulk Fermi level. The observations are compatible with a Fermi-level flat DOS, which of course does not demonstrate the DOS flatness. To illustrate this point, the charge density $\rho(E_d)$ has been computed using a dangling-bond Gaussian DOS, with a positive correlation energy of 0.4 eV, to describe the D^+ , D^0 , and D^- occupancies. Figure 7 shows the result of the calculation for two hypotheses of Gaussian widths $\sigma = 0.1$ and 0.2 eV, at room temperature. One observes

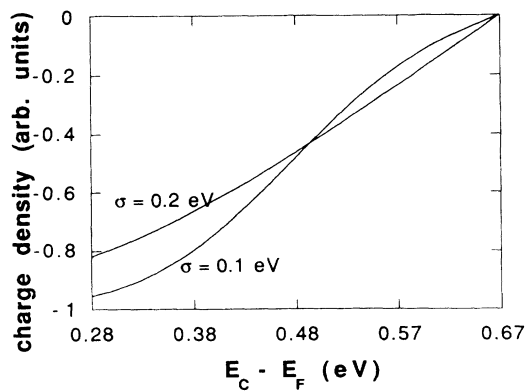


FIG. 7. Charge-density variation as a function Fermi-level position, assuming a Gaussian dangling-bond density of states, and an energy correlation of 0.4 eV. The Gaussian width is either 0.1 or 0.2 eV. The Fermi-level position corresponding to a null charge density is taken at 0.67 eV below the conduction band.

that in the domain of interest for $E_c - E_F$, both curves may fairly well be approximated by straight lines, which may be simulated using an effective flat DOS.

The observed absence of scaling is interpreted as due to the inclusion of diffusion in the transport equation, as already stated by Lampert and Mark.¹ Moreover, the present treatment of transport allows one to use boundary conditions at the n^+ - i interfaces more realistic than the ones required to derive scaling, namely zero electric field and infinite electron density at the injecting electrode. At high current densities, probably outside the range of experimental measurements, a scaling law is, however, predicted to hold. It corresponds to the situation where the distance between the electron band edge and the pseudo-Fermi level is constant through the intrinsic layer.

VI. CONCLUSION

The consideration of the effect of the space-charge region in computing the I - V characteristics of n^+ - i - n^+ α -Si:H sandwiches enables a fair description of the measurements performed on samples made of the same materials but with various thicknesses, using a unique DOS density. The value of this DOS density and its slope is severely constrained by the requirement to describe simultaneously the I - V measurements on thick and thin samples. The measurements exclude that the density of states varies exponentially with the energy in the Fermi-level vicinity. A hypothesis of energy-independent density of states is compatible with the observations. It is, however, shown that a Gaussian distribution of dangling bonds leads to a charge-density distribution depending approximately linearly on the value of the pseudo-Fermi level, just as a flat DOS does. So the present measurements are compatible with the commonly accepted vision of Gaussian dangling-bond DOS with a correlation energy of ≈ 0.4 eV and a width of 0.1–0.2 eV.

ACKNOWLEDGMENTS

We are indebted to I. Solomon, whose activity in SCLC has initiated the present study. We thank R. Vanderhaghen for helpful discussions on the determination of DOS by time-of-flight methods, and Ph. Delannoy for enlightening discussions on transport in polymers around the work of Bonham. The work was financially supported by PIRSEM-CNRS, AFME and CCE contract JOULE.

APPENDIX A

From time-of-flight experiments, one gets a relatively precise knowledge of the density of states below the conduction-band edge. Following Vanderhaghen and co-workers,^{11,12} we assume that the DOS has the following behavior.

From E_c to $E_1 = E_c - 0.15$ eV, it decreases exponen-

tially from $D_{cb} = 10^{21} \text{ cm}^{-3} \text{ eV}^{-1}$ at E_c with a characteristic energy of 0.026 eV. Under $E_c - 0.15$ eV, it decreases further with a characteristic energy $kT_1 = 0.017$ eV. The DOS around the Fermi level is not properly probed by time of flight, so one may assume that the DOS introduced to analyze SCLC measurements is to be added to the present ones.

The question arises of the contribution of these states to the charge density. 0-K approximation is not justified, for the characteristic energies are equal to or smaller than the thermal energy at the temperature of the measurements, ≈ 300 K, i.e., $kT = 0.026$ eV.

One may compute the contributions of these states to the charge density from the relation

$$\rho_1(E_F) = -qN_1 \int^{E_1} \exp\left(-\frac{E_1 - E}{kT_1}\right) \left[\frac{1}{1 + \exp\left(\frac{E - E_F}{kt}\right)} - \frac{1}{1 + \exp\left(\frac{E - E_{Fi}}{kT}\right)} \right] dE,$$

where $E_{Fi} \leq E_F \ll E_1$, N_1 is the DOS at $E = E_1$, and where

$$N_1 = D_{cb} \exp\left[-\frac{E_c - E_1}{kT}\right] \approx 3 \times 10^{18} \text{ cm}^{-3} \text{ eV}^{-1}.$$

With the particular choice of the ratio $kT/kT_1 = \frac{3}{2}$, here satisfied, this integral may be analytically evaluated, and one gets finally

$$\rho_1(E_F) \approx -2qkTN_1 \exp\left[-\frac{E_1 - E_F}{2kT}\right] \times \left[1 - \exp\left[-\frac{E_F - E_{Fi}}{kT}\right] \right].$$

The minimum value for $E_1 - E_F$ is 0.13 eV, at the $n^+ \text{-i}$ interfaces. There, one gets $1.3 \times 10^{16} \text{ cm}^{-3}$ elementary charges in these states, so they may contribute significantly to the SCLC characteristics.

The preceding expression for the charge density may be rewritten as a function of $u = \exp(E_d/kT)$, where $E_d = E_c - E_F$, convenient for the numerical evaluations. One gets

$$\rho_1(u) = -2qkTD_{cb} \exp\left[-\frac{E_c - E_1}{2kT}\right] u^{-1/2} \left[1 - \frac{u}{u_b} \right].$$

u_b is the value taken by u in a bulk material.

$$\rho(E_F) = -q \int g(E) \{f(E, E_F) - f(E, E_{Fi})\} dE.$$

$f(E, E_F)$ is assumed to be the Fermi-Dirac function, E_{Fi} is the bulk Fermi energy.

Note that $E_d = E_c - E_F$ is greater than or equal to $E_a^+ = 0.28$ eV, so that the pseudo-Fermi level is far enough from E_1 (recall that $E_c - E_1 = 0.15$ eV) to allow the use of the exponential approximation of the Fermi Dirac occupation probability function in the energy region between E_1 and E_c . One then gets easily the result that this part of DOS behaves like a DOS located at E_c with a density $N'_c = D_{cb}(E_c - E_1)$.

The charge-density contribution of the DOS at energies lower than E_1 is given by

APPENDIX B

The determination of $Y(u)$ from Eq. (6), valid in an interval (u_1, u_2) where $R(u)$ may be taken as constant and equal to R_a , leads to the resolution of

$$Y(u) - \ln[1 + Y(u)] = g(u), \quad (\text{B1})$$

where $g(u) = Y_2 - \ln(1 + Y_2) + (M^2/R_a)(u_2 - u)$ is a linear function of u .

Y_2 is assumed to be known from the treatment of the preceding interval, for the starting point is u_m the maximum value of u , where Z and therefore Y is known and equal to 0, and the end point is u_0 .

Two solutions are sought, one positive Y_+ , and the other negative Y_- , which turns out to be in our case always greater than -1 . Y_+ may be approximated by the expression

$$Y_+ \approx x + x^2 \frac{x+4}{x+6} \quad \text{where } x = \{2g(u)\}^{1/2}.$$

Similarly Y_- is approximated by the following expression, valid if $Y_- > -0.99$:

$$Y_- \approx x \frac{24 - 5x}{24 - 13x + 5x^2} \quad \text{where } x = -\{2g(u)\}^{1/2}.$$

From these approximations, an iteration procedure to solve Eq. (B1) was realized; it was checked that the approximations were accurate enough. The evaluation of the integral to get the thickness was then performed by quadrature of the above expressions.

- ¹M. A. Lampert and Mark, *Current Injection in Solids* (Academic, New York, 1970).
- ²J. Sworakowski and S. Nespurek, *J. Appl. Phys.* **65**, 1559 (1989).
- ³R. L. Weisfield, *J. Appl. Phys.* **54**, 6401 (1983).
- ⁴J. C. Van der Heuvel, R. C. Van Oort, B. Bokhorst, and M. J. Geerts, in *Amorphous Silicon Technology*, Proceedings of the MRS Spring Meeting, San Diego, 1989, edited by A. Madan, M. J. Thompson, P. C. Taylor, Y. Hamakawa, and P. G. Le Comber (Materials Research Society, Pittsburgh, 1989), p. 155.
- ⁵W. Den Boer, *J. Phys. (Paris) Colloq.* **42**, Suppl. 19, C4-451 (1981).
- ⁶I. Solomon, R. Benferhat, and H. Tran Quoc, *Phys. Rev. B* **30**, 337 (1984).
- ⁷J. S. Bonham, *Phys. Status Solidi A* **55**, 61 (1979).
- ⁸R. Meaudre, *Thin Solid Films* **148**, 121 (1987).
- ⁹R. Benferhat, thèse de doctorat d'Etat, Université Paris VI, 1983.
- ¹⁰A. C. Hourd and W. E. Spear, *Philos. Mag. B* **51**, L13 (1985).
- ¹¹R. Vanderhagen, *Phys. Rev. B* **38**, 755 (1988).
- ¹²C. Longeaud and R. Vanderhagen, *Philos. Mag. B* **61**, 277 (1990).
- ¹³A. Labdi, G. de Rosny, and B. Equer, *J. Non-Cryst. Solids* **144**, 399 (1989).
- ¹⁴A. Labdi, thèse de doctorat, Université Paris VII, 1988.